Algorithm Theoretical Basis Document (ATBD) of the CPP RDSAR processing for oceans

	Nom et Sigle	Date et Visa
Rédigé par	François BOY Thomas MOREAU (CLS)	
Accepté par	Nicolas PICOT	
Application Autorisée par	Nicolas PICOT	

Document géré en configuration : OUI/NON

CHRONOLOGY ISSUES

Version	Date	Objet
1.0	15/06/2013	Creation of ATBD Issue 1.0

SOMMAIRE

1. INTRODUCTION 4
1.1. Purpose and scope 4
1.2. Document structure 4

2. ACRONYMS LIST 4

3. OVERVIEW 5
3.1. References 7

4. ALGORITHM DESCRIPTION 9
4.1. Algorithm flow chart 9
4.2. Algorithm definition 10
4.2.1. To assemble 4 bursts 10
4.2.2. To correct the AGC for instrument errors 10
4.2.3. To compensate the echoes amplitude for the corrected AGC 10
4.2.4. To generate RDSAR echoes 10
4.2.5. To compute the tracker range and to correct the tracker ranges for the USO frequency drift 11
4.2.6. To apply the internal path correction 11
4.2.7. To correct the tracker range for the Doppler correction 11
4.2.8. To correct the waveforms from low-pass filter mask 11
4.2.9. Retracking 12
4.2.10. To compute the backscatter coefficients 12
4.3. Known limitations and their implications 12
4.4. References 13

1. INTRODUCTION

1.1. PURPOSE AND SCOPE

This document is the Algorithm Theoretical Basis Document (ATBD) for the methods and algorithms used to derive the CryoSat-2 RDSAR L2 products for Open Ocean, as defined within the Cryosat Processing Prototype (CPP) from CNES. This document provides the scientific background of the algorithms.

1.2. DOCUMENT STRUCTURE

This document is structured into an introductory chapter followed by two chapters describing the the background (section 2) of this product development and the two-step algorithm (section 3), namely

- The L1b processing: reducing SAR mode data into 20-Hz pulse limited altimeter data,
- The retracking: a conventional Brown ocean retracker is applied to the reduced SAR-mode data for retrieving the different geophysical parameters.

A short description of the proposed approach is done within the document. The capabilities and limitations of the algorithms are also discussed.

2. ACRONYMS LIST

ATBD	Algorithm Theoretical Basis Document
BRF	Burst Repetition Frequency
CPP	Cryosat Processing Prototype
FAI	Fine Altitude Instruction
FBR	Full Bit Rate (un-calibrated, geo-located I and Q individual echoes in time domain)
LRM	Low Resolution Mode
NA	Not Applicable
NRT	Near Real Time
POD	Precise Orbit Determination
PTR	Point Target Response
RD	Reference Document
RDSAR	Reduces Synthetic Aperture radar
RIR	Range Impulse Response
SAR	Synthetic Aperture radar
SIRAL	Synthetic Aperture Interferometric Radar Altimeter
SLA	Sea level Anomalies
SSB	Sea State Bias
TAI	International Atomic Time
USO	Ultra-Stable Oscillator

3. OVERVIEW

The CryoSat-2 radar altimeter (SIRAL) has three operating modes: the Low Resolution Mode (LRM), the SAR mode and the SARIn mode. For the SAR mode, in contrast to the LRM, the altimeter is transmitting pulses in groups (bursts), of 64 pulses at high PRF (18.182 kHz), with a burst repetition frequency (BRF) of 85.7 Hz [Wingham et al., 2006]. The closed-burst timing is shown in Figure 2.1. The PRF is about 10 times higher than that of LRM, which inherently ensures a high level of phase coherence from pulse to pulse within the burst. The returning echoes are thus correlated making them suitable for azimuth processing (SAR). The 128, I and Q, time domain samples of each individual echo are directly telemetered to ground for SAR processing then geo-located to form the FBR data.

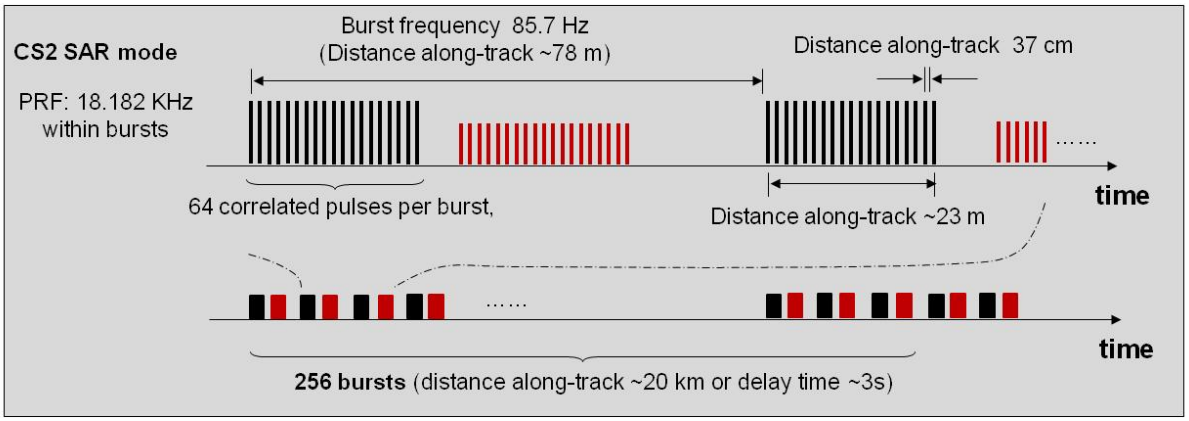

Figure 2.1: SIRAL transmission and reception timing in SAR-mode.

Though the along-track improvement in sampling resolution is straightforward, it still remains some uncertainties in the SAR retrieved elevations as well as the other surface parameters accuracies. To allow the assessment of the in-orbit performances of the SAR mode data and in the same manner the quality of the processing method, CNES has developed a reduced SAR (RDSAR) methodology [Boy et al., 2012] that aims at emulating LRM echoes, similar to the conventional pulse limited waveforms, from SAR mode data to make quantitative comparisons of their measurements over identical sea state.

Figure 2.2 illustrates the differences in footprint geometry between the conventional pulse limited altimeter and the SAR altimeter: the footprint of a conventional altimeter is pulse-limited whereas the SAR altimeter uses the Doppler principle to achieve a small along-track footprint. The resulting RDSAR and SAR power thus have an important distinction. Figure 2.2 shows the differences in the received echoes from a conventional altimeter (here a RDSAR waveform) and the SAR altimeter (waveform with a steep leading edge and fast decay trailing edge).

To ease the comparison, SAR and RDSAR CPP echoes are generated at the same along-track location allowing both retrievals to be directly subtracted without the need to apply any geophysical model (e.g., wet and dry troposphere correction, ionosphere correction, tidal correction, dynamic atmospheric correction) or orbit elements (like the orbital ephemerides to derive a precise altitude or also to align CryoSat-2 with other missions) that may contribute to differences and lead to unclear conclusions regarding the comparison between the different processing approaches. This is especially true for the sea level anomaly (SLA) and other altimeter derived products like the wind measurements that account for corrections and/or models.

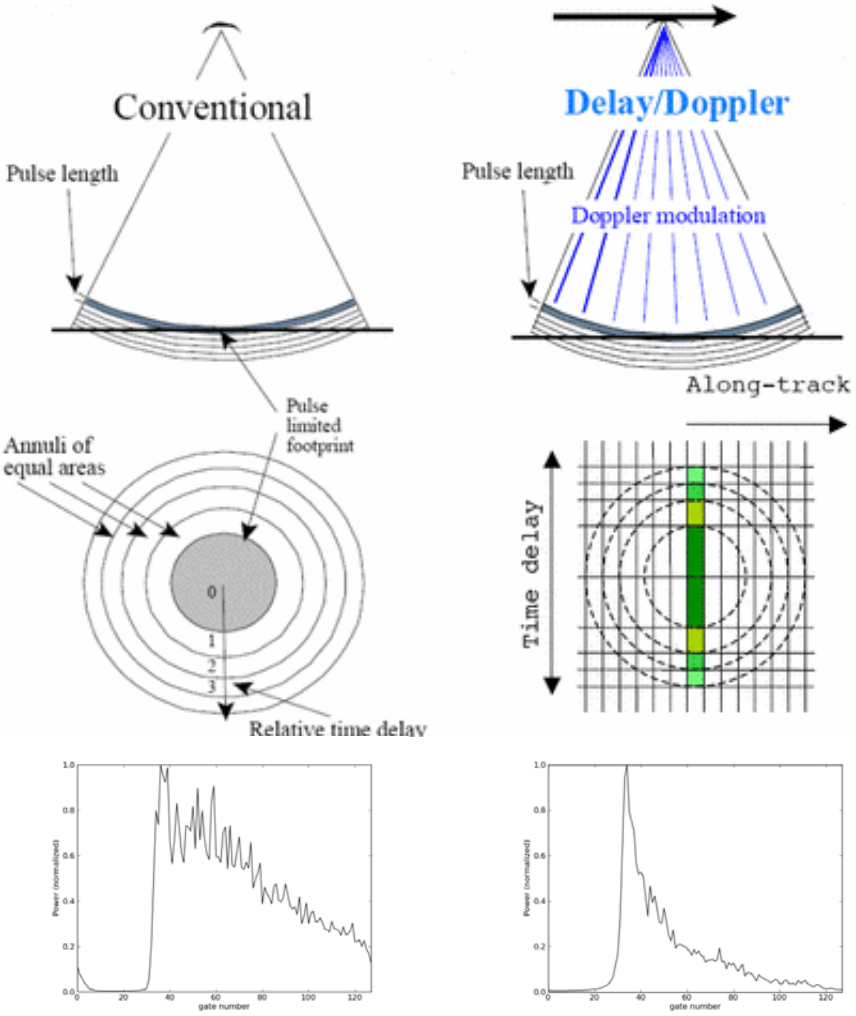

Figure 2.2: Comparison of the footprint geometry between (left panels) LRM conventional radar altimeter and (right panels) Delay/Doppler SAR altimetry (Credits R.K. Raney, Johns Hopkins University, Applied Physics Laboratory) and example of reduced-SAR waveform and its collocated multi-looked echo power from CPP (lower panel).

In SAR mode 4 bursts per 20 Hz tracking cycle are transmitted. Thus when SAR data are processed in a pulse-width limited manner (RDSAR), the timing and number of pulses per unit time is different to the LRM sequence of a conventional altimeter (90 independent pulses regularly spaced per tracking cycle). The CPP RDSAR method uses 256 echoes per tracking cycle (i.e. all the echoes from pulses contained within 4 successive SAR bursts). As in LRM mode, echoes are then power detected and accumulated to form a 20 Hz Brown echo. However a much smaller number of pulses are contributing to the range noise reduction of the resulting waveform, since significant pulse-to-pulse correlations are obtained at the PRF of 18 kHz (Figure 2.3). Only 32 pulses, corresponding to a ~2 kHz frequency, are contributing to the speckle de-correlation instead of 90 for Cryosat-2 LRM for weak SWH, which leads to a noisy RDSAR waveforms and, thereby, a retrieved range error multiplied by a factor of sqrt(90/32) for comparison with LRM one. In practice by using all echoes, not merely every 9th one, the overall noise performance is slightly further improved since pulse de-correlation (notably by thermal noise and for higher significant wave heights) occurs in reality at higher PRF than the 2 kHz that is suggested by Walsh's theory [Smith et al., 2012].

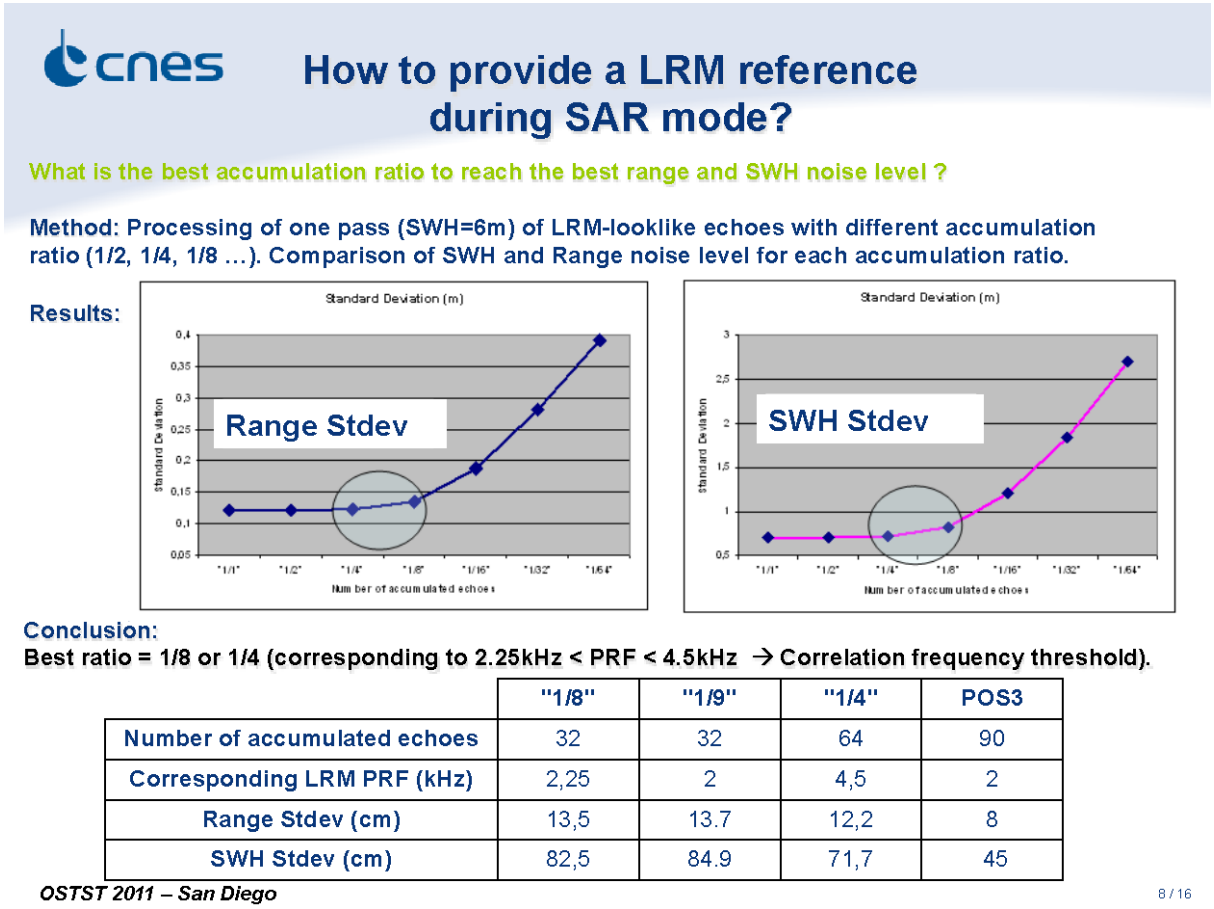

	"1/8"	"1/9"	"1/4"	POS3
Number of accumulated echoes	32	32	64	90
Corresponding LRM PRF (kHz)	2,25	2	4,5	2
Range Stdev (cm)	13,5	13.7	12,2	8
SWH Stdev (cm)	82,5	84.9	71,7	45

Figure 2.3: Accumulation taking every 9th echo provides efficient reduction of the speckle noise (from Boy et al., 2011).

Another key objective of the RDSAR methodology was to build and maintain the data quality continuity between SAR and LRM modes. It is hence important to ensure that the RDSAR data are fully consistent and valuable to be considered as a well-known LRM reference during SAR mode.

3.1. REFERENCES

[Wingham et al., 2006]: D. J. Wingham, C. R. Francis, S. Backer, C. Bouzinac, D. Brockley, R. Cullen, P. de Chateau-Thierry, S. W. Laxon, U. Mallow, C. Mavrocordatos, L. Phalippou, G. Ratier, L. Rey, F. Rostan, P. Viau, D. W. Wallis, "*CryoSat: A Mission to determine the Fluctuations in Earth's Land and Marine Ice Fields*", Advances in Space Research, Vol. 37, Jan. 2006, Issue 4, pp.841-871.

[Boy et al., 2012]: F. Boy, T. Moreau, J-D. Desjonquères, S. Labroue, N. Picot, J-C. Poisson and P. Thibaut, *"Cryosat Processing Prototype, LRM and SAR Processing"*, presented at the 2012 Ocean Surface Topography Science Team Meeting. Available online: http://www.aviso.oceanobs.com/fileadmin/documents/OSTST/2012/oral/02_friday_28/02_instr_processing_II/02_IP2_Boy.pdf

[Boy et al., 2011]: F. Boy, J-D. Desjonquères and N. Picot, *"Cryosat Processing Prototype (CPP), CRYOSAT LRM, TRK and SAR Processing"*, presented at the 2011 Ocean Surface Topography Science Team Meeting. Available online: http://www.aviso.oceanobs.com/fileadmin/documents/OSTST/2011/oral/01_Wednesday/Splinter%201%20IP/06%20%20Boy%20CPP%20Presentation.pdf

[Smith et al., 2012]: W. Smith and R. Scharroo, "*Pulse-to-pulse correlation in CryoSat SAR echoes from ocean surfaces: implications for optimal pseudo-LRM waveform averaging*", presented at the 2012 Ocean Surface Topography Science Team Meeting. Available online: http://www.aviso.oceanobs.com/fileadmin/documents/OSTST/2012/oral/02_friday_28/05_instr_processing_IIb/03_IP2B_Smith1.pdf

4. ALGORITHM DESCRIPTION

4.1. ALGORITHM FLOW CHART

The description of the algorithm in the subsequent sections is facilitated by the flow chart shown in Figure 3.1, which outlines the key parts in the way the algorithm works.

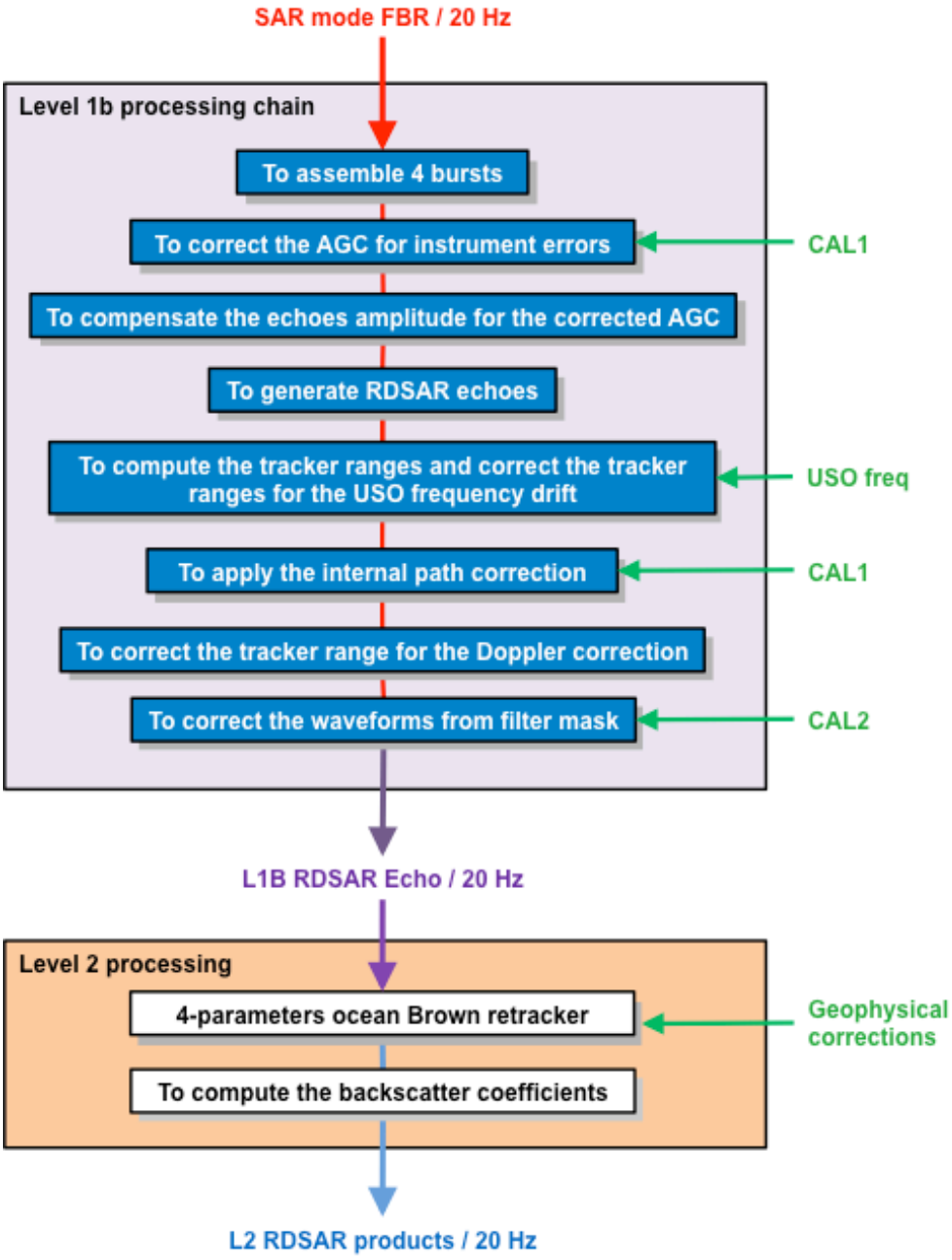

Figure 3.1: Flowchart showing the sequence of operations performed by the RDSAR processing scheme

4.2. ALGORITHM DEFINITION

In this section, a definition of the different block algorithms is given. They are listed in an order that follows the RDSAR processing scheme.

4.2.1. TO ASSEMBLE 4 BURSTS

The FBR data form the input to the full RDSAR processing. It is the highest level data in which the full information content of the acquired data is retained. At this stage, the individual echoes are complex-valued, I and Q, data at high pulse repetition frequency, that are not calibrated, but deramped in time domain, and tagged with time and geolocation.
For each 20 Hz tracking cycle, 4 bursts of 64 echoes are processed through the L1b RDSAR processing chain simultaneously.
The obtained 20 Hz RDSAR data are assigned a time tag that corresponds to the time at the center of the 4 bursts. In turn, this time is corrected for a one-way satellite-to-surface travel of a radar wave in order to get the time corresponding to when the pulse hits the Earth surface. The 20 Hz point positions on the Earth surface are defined by the sub-satellite point location (the nadir point) at this time.

4.2.2. TO CORRECT THE AGC FOR INSTRUMENT ERRORS

An internal calibration monitors the instrument Range Impulse Response (RIR), like traditional altimeters, to identify any gain variation in the Transmitter/Receiver chain with respect to the nominal condition characterized on ground, which may be caused by some small instrument power changes during flight. This amplitude correction is related to the power level drift of this RIR. It is extracted from CAL1, and then added to the on-board AGC measurements (AGC1 and AGC2) to obtain the corrected AGC value *AGC_total*.

4.2.3. TO COMPENSATE THE ECHOES AMPLITUDE FOR THE CORRECTED AGC

This function applies the corrected AGC value to the complex raw echoes (*Wf_I_raw +jWF_Q_raw*), as follows:

$$Wf\_I(n) = Wf\_I\_raw(n)/\sqrt{10^{\frac{AGC_{total}}{10}}}$$

$$Wf\_Q(n) = Wf\_Q\_raw(n)/\sqrt{10^{\frac{AGC_{total}}{10}}}$$

n being the sample number of the echoes in the time domain (from 0 to 127)

The amplitude of each individual complex echo is scaled accordingly.

This function is inherited from the SAR processing chain, and has been kept for convenience in the RDSAR chain too (even if the AGC setting is held constant during a tracking cycle of 4 bursts).

4.2.4. TO GENERATE RDSAR ECHOES

The purpose of this stage is to compute the LRM-like power waveforms from SAR mode pulses.

In a tracking cycle of 4 bursts, the 4*64 complex echo profiles may vary of position inside the range window due to the varying distance between the satellite and the Earth surface around its orbit.

Consequently, those individual echoes need to be first all aligned on the same reference gate before the averaging step is performed.

On-board, the altimeter performs a partial alignment of the echoes (in order to build the tracking echo). The (I,Q) echoes, as available in telemetry or FBR data, are corrected for the Burst to Burst shift but the shift inside the Burst is not managed. Moreover, the range shift is calculated from an on-board pre-computed radial velocity (COR2), which is very noisy.

So, the proposed method consists of:

1 – Undoing the partial alignment performed by the altimeter (using COR2 command)

2 - Applying a finer shift to the I and Q echo profiles, to make them aligned to a reference position corresponding to the first echo of the cycle, using the precise radial velocity provided by the orbit ephemeris (MOE or POE).

For each individual complex echo, the phase shift corresponding to the distance shift can then be written as:

$$\phi(n,t) = \exp(-2j\pi * \delta f * t)$$

where δf is the needed frequency translation, n the pulse number and t the time or abscissa of the time domain echoes.
We apply the phase compensation term to each I and Q echoes converted in time domain by a fast fourier transform (FFT).
For each of the 4*64 echoes (I and Q) corrected for distance, a 128-points FFT is performed and the I2+Q2 spectrum is derived. The 20 Hz Pseudo-LRM 128-points I2+Q2 spectrum is then computed by summing the 4*64 I2+Q2 waveforms.

4.2.5. TO COMPUTE THE TRACKER RANGE AND TO CORRECT THE TRACKER RANGES FOR THE USO FREQUENCY DRIFT

The tracker range is computed from the tracker range command of the corresponding cycle.

Then, as the RDSAR echo has been built using the first pulse of the cycle as a reference and as the measurement is time-tagged at the center of the cycle, the tracker range is corrected for a distance corresponding to the radial satellite movement during half cycle duration.

To finish, the Ultra-Stable Oscillator (USO) clock period is needed to accurately convert the range delay counter values into time units (and then spatial units) in order to derive the altimeter range. Some USO clock period variations (USO drift) may occur due to the ageing of the device and cause some error in range.

The correction is regularly updated in the ground processing via an auxiliary file. It is to be added to the altimetric retracked range.

4.2.6. TO APPLY THE INTERNAL PATH CORRECTION

The monitoring of the whole RIR shape is also performed to correct any range drift due to the offset of the RIR position with respect to the 0-frequency, accounting for instrumental evolutions.

This internal path correction extracted from CAL1 is to be added to the altimetric retracked range on ground.
This function is traditionally used in conventional altimetry. But the CPP RDSAR processing does not apply the internal path delay because this correction is a constant bias, identical for each mode (SAR, LRM and RDSAR). So, we can correctly cross compare each mode even if this correction is not applied.

4.2.7. TO CORRECT THE TRACKER RANGE FOR THE DOPPLER CORRECTION

The tracker range is corrected for the Doppler correction, caused by the Doppler shift in the line of sight to the nadir direction.

4.2.8. TO CORRECT THE WAVEFORMS FROM LOW-PASS FILTER MASK

A specific in-flight calibration mode allows the computation of the instrument filter mask needed to correct the echo waveform from the thermal noise effects. It is obtained by accumulation of the noise spectra within the bandwidth of interest, which is then normalized and inverted to form the filter mask shape.

The *Filter* correction extracted from CAL2 (filter mask file) is to be applied to the averaged altimeter echo samples *Wf_Ampl_Raw* on ground. However, a unique filter is employed within the current CPP processing chain for this purpose.

The corrected waveform *Wf_Ampl* may be retrieved by:

$$Wf\_Ampl(n) = \frac{Wf\_Ampl\_Raw(n)}{Filter(n)}$$

n being the sample number of the echoes in the time domain (from 0 to 127)

4.2.9. RETRACKING

A conventional Brown ocean retracker based on unweighted least square estimations (also known as MLE) which are traditionally used with LRM echoes [Amarouche et al., 2004], is applied to the RDSAR power waveforms for retrieving the different geophysical parameters (range, significant wave height, backscattering coefficient). A 4-parameter estimator is considered for adequately fitting the measured waveforms with the return power model since the CryoSat-2 satellite exhibits unstable off-nadir mispointing angle in flight. These parameters are then corrected to account for the Gaussian approximation of the PTR in the retracking algorithm scheme, the ellipticity of the CryoSat-2 antenna, and its particular speckle reduction property (different from conventional altimetry mode), through pre-computed Look-Up correction Tables (LUT). This correction depends on the wave height and could be as high as 1 cm in range and 20 cm in wave.

Some additional altimeter components are needed to be used in the Sea Level Anomalies (SLA) calculation as defined by this formula:

$$SLA = Orbit - Range - \sum_{i=0}^{N} C_i - MSS$$

where *Orbit* corresponds to the distance between the satellite and the ellipsoid, *Range* is the distance measured by the altimeter between the satellite and the sea surface, *MSS* is the Mean Sea Surface of the ocean over a long period and $\sum_{i=0}^{N} C_i$ is the sum of all the corrections needed to take into account the atmospherically effects (wet and dry troposphere, ionosphere, inverse barometer) and the geophysical phenomena (ocean tides, high frequency atmospheric effects on ocean).

Note that the sea-surface state (electromagnetic sea-surface bias) is not considered in the equation since no SSB solution has been calculated yet.

4.2.10. TO COMPUTE THE BACKSCATTER COEFFICIENTS

For each averaged measurement, the 20 Hz Sigma0 is computed by combining the retracked amplitude of the waveforms with the scaling factors, as follows:

$$\sigma_0 = 30 * log_{10}(Orbit\_Alt) + 10 * log_{10}(Earth\_Rad + Orbit\_Alt) + 10 * log_{10}(Pu) + constant$$

4.3. KNOWN LIMITATIONS AND THEIR IMPLICATIONS

Known limitations and shortcomings of these methods and algorithms:

- Due to the processing method implemented by CNES, a data gap of 2.5 seconds occurs in the RDSAR data set at the transition between LRM and SAR mode, such impacting our analysis of the LRM/RDSAR continuity.
- One feature of the CryoSat-2 satellite is its significant mis-pointed antenna and elliptical antenna pattern. While the theory of pulse-limited echoes from mis-pointed antenna is well known (a second order model of the altimeter waveform is developed for mispointing angle values up to 0.7° [Amarouche et al., 2004]), the ellipticity of the antenna differs from earlier pulse-limited system (circular). For elliptical pattern (like SIRAL), the altimeter echo model has to be modified to take into account this new instrument characteristic. After modifying accordingly the ocean analytical retracking algorithm, some comparisons have been performed with a numerical retracker that mimics this new geometry. Results have been found quite similar so that it validates the use of the corrected analytical retracker.
- The speckle reduction performance of the reduced SAR approach is not as efficient as for the conventional altimeter pulse-limited resolution mode. Due to this higher measurement noise, the RDSAR echo shape is slightly different to the LRM one, leading to discrepancies in the way the model fits the echo over identical sea state. Appropriate look-up tables have to be computed to

take into account this effect and correct the estimations (range, significant waveheight, sigma0 and mispoiting angle) issued from an ocean analytical retracking algorithm.

The mentioned limitations will be addresses and improved in future versions of the CPP products.

4.4. REFERENCES

[Amarouche et al., 2004]: L. Amarouche, P. Thibaut, O.Z. Zanife, J.-P. Dumont, P. Vincent and N. Steunou, "*Improving the Jason-1 ground retracking to better account for attitude effects*", marine Geodesy, Vol. 27, pp.171-197, 2004.

DIFFUSION

NOM	SIGLE/SOCIETE	NB	NOM	SIGLE/SOCIETE	NB
François BOY	CNES		Nicolas PICOT	CNES	
Jean-Damien Desjonqueres	CNES		Sophie COUTIN-FAYE	CNES	
Thomas Moreau	CLS				
Pierre Thibaut	CLS				